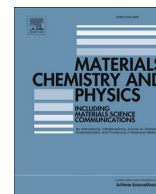




Contents lists available at ScienceDirect

## Materials Chemistry and Physics

journal homepage: [www.elsevier.com/locate/matchemphys](http://www.elsevier.com/locate/matchemphys)

## Modification of photosensing property of CdS–Bi<sub>2</sub>S<sub>3</sub> bi-layer by thermal annealing and swift heavy ion irradiation

Shaheed U. Shaikh<sup>a, b</sup>, Farha Y. Siddiqui<sup>a, b</sup>, Fouran Singh<sup>c</sup>, Pawan K. Kulriya<sup>c</sup>, D.M. Phase<sup>d</sup>, Ramphal Sharma<sup>a, b, \*</sup>

<sup>a</sup> Thin Film and Nanotechnology Laboratory, Department of Physics, India

<sup>b</sup> Department of Nanotechnology, Dr. Babasaheb Ambedkar Marathwada University, Aurangabad 431004, India

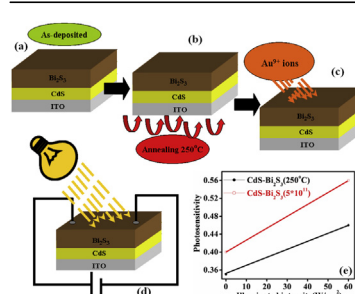
<sup>c</sup> Inter University Accelerator Center, Aruna Asaf Ali Marg, New Delhi 110 067, India

<sup>d</sup> UGC DAE Consortium for Scientific Research, Khandwa Road, Indore 452017, India

### HIGHLIGHTS

- CdS–Bi<sub>2</sub>S<sub>3</sub> bi-layer thin film prepared at room temperature.
- Irradiated using Au<sup>9+</sup> ions at the fluence of  $5 \times 10^{11}$  ion/cm<sup>2</sup> with 120 MeV energy.
- Study of modification induced by irradiations.
- Study of Photosensitivity after annealing and irradiation.

### GRAPHICAL ABSTRACT



### ARTICLE INFO

#### Article history:

Received 11 May 2015

Received in revised form

19 September 2015

Accepted 5 November 2015

Available online xxx

#### Keywords:

Semiconductors

Chemical synthesis

Annealing

Optical properties

Electrical properties

### ABSTRACT

The CdS–Bi<sub>2</sub>S<sub>3</sub> bi-layer thin films have been deposited on Indium Tin Oxide (ITO) glass substrates at room temperature by Chemical Bath Deposition Technique (CBD) and bi-layer thin films were annealed in air atmosphere for 1 h at 250 °C. The air annealed sample was irradiated using Au<sup>9+</sup> ions at the fluence  $5 \times 10^{11}$  ion/cm<sup>2</sup> with 120 MeV energy. Effects of Swift Heavy Ion (SHI) irradiation on CdS–Bi<sub>2</sub>S<sub>3</sub> bi-layer thin films were studied. The results are explained on the basis annealing and high electronic excitation, using X-ray diffraction (XRD), Selective Electron Area Diffraction (SEAD), Atomic Force Microscopy (AFM), Raman Spectroscopy, UV spectroscopy and I–V characteristics. The photosensing property after illumination of visible light over the samples is studied. These as-deposited, annealed and irradiated bi-layer thin films are used to sense visible light at room temperature.

© 2015 Published by Elsevier B.V.

### 1. Introduction

Cadmium sulphide (CdS) and Bismuth sulphide (Bi<sub>2</sub>S<sub>3</sub>) is n-type

semiconductor, which belongs to II–VI and V–VI group with wide direct band gap 2.48 eV and 1.78 eV, respectively. The mentioned qualities make CdS and Bi<sub>2</sub>S<sub>3</sub> potentially suitable for fabrication of optoelectronic devices as well as applications in solar cell fabrication [1–3] photosensor [4] and thermoelectric power [5–7]. CdS and Bi<sub>2</sub>S<sub>3</sub> thin film are the most sensitive semiconductors well-known today, especially for conversion of visible and near

\* Corresponding author. Department of Nanotechnology, Dr. Babasaheb Ambedkar Marathwada University, Aurangabad 431004, India.

E-mail address: [ramphalsharma@yahoo.com](mailto:ramphalsharma@yahoo.com) (R. Sharma).

infrared radiations into electrical energy at room temperature [8,9]. Only few reports are available in literature on bi-layer thin film followed by annealing and irradiation like Sb–Se bi-layer [10] and zinc ferrite-FeNiMoB alloy based bi-layer film [11]. The concept of bi-layer thin film is one of the interesting areas for researchers to produce new class of sensor. The preparation of the bi-layer thin film is quite challenging by cost effective chemical synthesis at room temperature. The authors have not come across any studies in bi-layer of CdS–Bi<sub>2</sub>S<sub>3</sub>. There are also probabilities to generate new properties which are distinct from the original material and may enhance the original properties of the material. The prepared bi-layer thin film can be further modified by various post deposition techniques like doping, annealing in different atmospheres and irradiation by various ions.

The purpose of present investigation is to deposit the CdS–Bi<sub>2</sub>S<sub>3</sub> bi-layer thin film by low cost CBD technique at room temperature and study the modifications created as a result of air annealing and 120 MeV Au<sup>9+</sup> ion irradiation on samples and its effect on performance of photosensing property at room temperature for photo-sensor applications.

## 2. Experimental details

All the chemicals used in experiment procedure were analytical pure, and were used without further purification. In typical preparation of the samples Cadmium sulfate hydrate CdSO<sub>4</sub>·8H<sub>2</sub>O (0.02 M), Thiourea (CS (NH<sub>2</sub>)<sub>2</sub>) (0.03 M) and Ammonia (5 mL) were introduced into distilled to give final concentrations and final volume of solution was 25 (mL). The chemically cleaned ITO glass substrate is dipped vertically in the solution for 3–4 h. Uniform thin film of CdS was deposited on ITO glass substrate by CBD technique. Thickness of CdS thin film is found to be ~350 nm. Sequentially Bi<sub>2</sub>S<sub>3</sub> thin film was grown on the CdS thin film at room temperature. The CdS thin film is dipped in bismuth and sulfide solution for 20 cycles. Bismuth nitrate GR (Bi(NO<sub>3</sub>)<sub>3</sub>·5H<sub>2</sub>O) (0.003 M) and Thioacetamide (C<sub>2</sub>H<sub>5</sub>NS) (0.1 M) were used as source of bismuth and sulfide, respectively. The pH of the solution was maintained with the Hydrazine hydrate. Bi<sub>2</sub>S<sub>3</sub> thin film was deposited by Successive Ionic Layer Adsorption and Reaction (SILAR) technique. The homogeneous thin film of Bi<sub>2</sub>S<sub>3</sub> of thickness ~200 nm was obtained over the CdS thin film. Finally the CdS–Bi<sub>2</sub>S<sub>3</sub> bi-layer thin film of thickness ~550 nm was deposited over ITO glass substrate. Further prepared bi-layer thin films were annealed in air atmosphere at 250 °C for 1 h. Annealed samples were cut into 1 × 1 cm<sup>2</sup> area used as target in the irradiation experiment.

### 2.1. Swift heavy ion irradiation

The use of SHI for material modifications is an efficient post deposition treatment, which enables control on compositional and surface modification in the material. In this process, an ion impinged on the surface of the thin film loses its energy in the form of inelastic collisions, which may be used for the excitation of electrons from their atomic levels in the material.

Irradiation causes loss in energy by two different independent processes, through nuclear energy loss (S<sub>n</sub>) and electronic energy loss (S<sub>e</sub>). The effect of electronic stopping power (S<sub>e</sub>) dominates over nuclear stopping power (S<sub>n</sub>) [12,13].

The electronic energy loss is responsible for the inelastic collision in which the atoms of target get excited or ionized. These inelastic collisions result in ionization of the charge carriers and atoms from their molecular levels, which make drastic change in the material by displacing ions from the surface and mixing at an interface. These ionic displacements create vacancies and defects in the material along with creation of ion tracks which may

correspond to the surface modifications. This process leads to the formation of point defects, phase transformation, crystallization and amorphization [14,15].

The irradiation experiments were performed on the 15 UD tandem Pelletron at IUAC, New Delhi, India. The thin film was irradiated by 120 MeV Au<sup>9+</sup> ions with 5 × 10<sup>12</sup> ions cm<sup>-2</sup> fluence. The average electronic energy loss (S<sub>e</sub>) for 120 MeV Au<sup>9+</sup> ions in CdS–Bi<sub>2</sub>S<sub>3</sub> matrix was calculated using the Monte Carlo Code TRIM-2010. The average electronic energy loss (S<sub>e</sub>) was found 2.189 keVÅ<sup>-1</sup> in CdS–Bi<sub>2</sub>S<sub>3</sub> bi-layer thin film. Fig. 1 indicates the electronic energy loss is the dominant mechanism through the gold ions which loses their energy in CdS–Bi<sub>2</sub>S<sub>3</sub> bi-layer thin film through electronic excitation.

### 2.2. Characterization of CdS–Bi<sub>2</sub>S<sub>3</sub> thin films

As-deposited, air annealed and irradiated CdS–Bi<sub>2</sub>S<sub>3</sub> bi-layer thin films were characterized using several techniques. The thickness of the film was determined by weight gravimetric method, using the density value as 4.82 g/cm<sup>3</sup> for CdS and 7.7 g/cm<sup>3</sup> for Bi<sub>2</sub>S<sub>3</sub> respectively. The phase and structural investigation were carried out on Bruker AXS X-ray diffractometer, Germany (Model D8Advanced) using Cu-K<sub>α</sub> radiation of λ = 1.5406 Å in the detector scan mode, with in the range of 20–60°. Topography of the thin film samples were studied by Atomic force microscopy (AFM) of Digital/Veeco Instrument Inc. Optical study performed by Perkin Elmer, Lambda 25 spectrophotometer within the range 300–1100 nm. Raman spectra in the region 100 to 750 cm<sup>-1</sup> of the samples were recorded by Raman molecular spectroscopy from Renishaw UK. Finally, I–V measurements were studied by Lab Equipment model interface with computer by applying silver contacts over the thin film and the results are presented.

## 3. Results and discussion

### 3.1. Structural studies

The XRD patterns of as-deposited, air annealed and Au<sup>9+</sup> ion irradiated CdS–Bi<sub>2</sub>S<sub>3</sub> bi-layer thin films are shown in Fig. 2. The high intense peaks in XRD diffraction pattern corresponds to the characteristics peak of ITO glass substrate. The X-ray diffraction

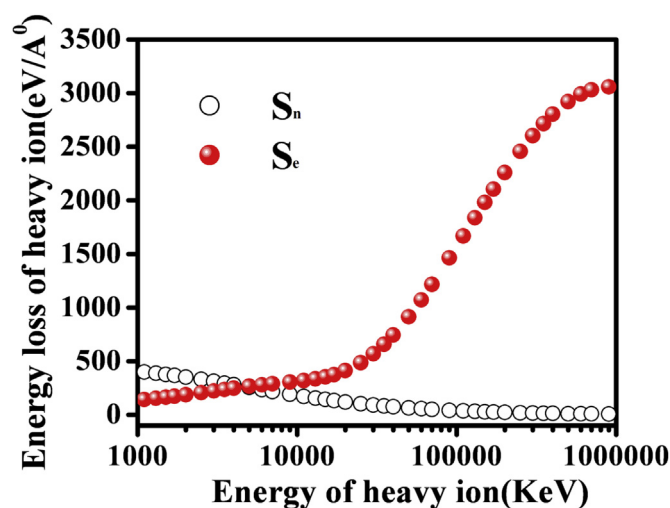


Fig. 1. Schematic of variation in electronic and nuclear energy loss of 120 MeV Au<sup>9+</sup> ions in CdS–Bi<sub>2</sub>S<sub>3</sub> thin films as a function of ion energy in CdS and inset for Bi<sub>2</sub>S<sub>3</sub> respectively.

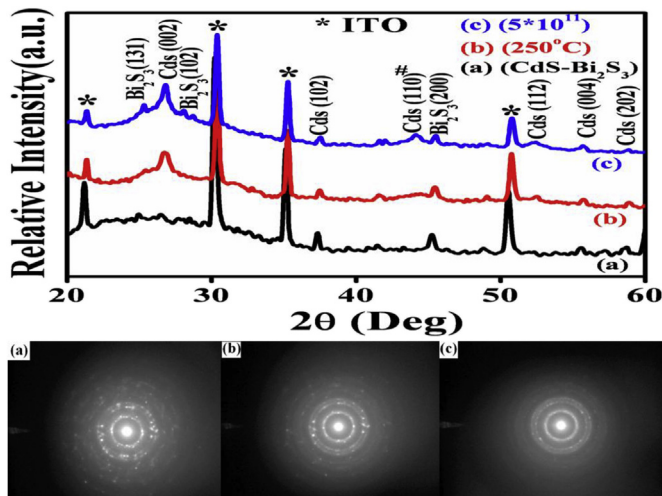


Fig. 2. XRD pattern and SEAD pattern of as-deposited, 250 °C air annealed and irradiated at fluence  $5 \times 10^{11}$  ion/cm<sup>2</sup> thin film of CdS–Bi<sub>2</sub>S<sub>3</sub> bi-layer.

pattern exhibit peaks of Bi<sub>2</sub>S<sub>3</sub> at 25.30°, 28.11°, 45.33° and 49.02° corresponding to the (1 3 1), (1 0 2), (2 0 0), (0 1 6), and (0 0 4) planes of orthorhombic phase. Whereas, the peaks of CdS were observed at 26.79°, 37.54°, 52.41°, 55.60° and 59.02° can be assigned to (0 0 2), (1 1 2), (0 0 4), (0 1 6), and (2 0 2) planes of hexagonal phase. Lattice parameters can be calculated with help of following relation.

$$\frac{1}{d^2} = \frac{4}{3} \left( \frac{h^2 + hk + k^2}{a^2} \right) + \frac{l^2}{c^2}$$

The calculated lattice parameters are in agreement with the JCPDS data (84–0279 and 80–0006).

The average crystallite size has been calculated from the X-ray diffraction pattern considering prominent peaks of CdS and Bi<sub>2</sub>S<sub>3</sub> by using the Debye-Scherrer's formula.

$$D = \frac{k\lambda}{\beta \cos \theta}$$

where, D is the crystallite size, K is shape constant and is equal to 0.94;  $\beta$  is the full width at half maximum (FWHM) and  $\lambda$  is the wavelength of the X-rays. The calculated average crystallite size of as-deposited thin film is found to be 12 nm and increases to 20 and 30 nm for annealed and irradiated samples, respectively.

The dislocation densities are calculated by  $\delta = 1/D^2$  [12,15] where as D is average crystallite size. The calculated values are  $6.94 \times 10^{15}$ ,  $2.50 \times 10^{15}$  and  $1.111 \times 10^{15} \text{ m}^{-2}$  for as-deposited, air annealed and irradiated samples respectively. The bi-layer thin film is stable against the irradiation. The  $2.189 \text{ keV}\text{\AA}^{-1}$  electronic loss might not be sufficient for amorphization of bi-layer thin film. The peaks became sharper and FWHM decreases in case of annealing as result of agglomeration [13,16]. The electronic excitation in thin film through energetic releases strain between the grains and shifts the interplanar spacing towards stress free value [14,17]. Irradiation enhances average crystallite size and the structure is found to be improved [18–20].

The estimated value of  $\delta$  shows decrease in dislocation density values. Inset figures (a), (b) and (c) represents SEAD pattern of as-deposited annealed and irradiated thin film respectively. SEAD images shows ring pattern which conforms polycrystalline nature of prepared bi-layer thin films [21]. The improvement in ring pattern can be correlate with crystallite size. In our case study the

average crystallite found to be improved after annealing and irradiation which is well agreement with XRD results.

### 3.2. Surface topography studies

The surface topography of samples is analyzed by atomic force microscopy through tapping mode. Fig. 3 (a), (b) and (c) shows two dimensional AFM images for as-deposited, annealed and irradiated samples, respectively. Fig. 3 (a) shows formation of small size large number of the grains over ITO glass substrate. The agglomeration of grain is mainly attributed to annealing of the sample. Annealing involves heating and controlled cooling of material to increase the size of the crystal and rearrange them periodically to reduce the defect. This process causes the conversion of small grains into cluster or larger grains [13,22]. The process of agglomeration is clearly observed in Fig. 3 (b). Irradiated sample shows the enlarge grains with complete and well defined grain boundaries. During irradiation process the kinetic energy of the electrons ejected from the target atom is transferred to lattice by electron phonon interaction which increases local lattice temperature over the melting point of the material. The melted grains coalesce with each other and forming larger grain. We assumed that heat gets confined with in grain volume. This increases the volume of grain resulting in grain agglomeration over the surface [23]. The formation of larger grains is shown in Fig. 3(c). The roughness of the samples is found to be changed from 98 to 123.60 and 175.54 nm for as-deposited, annealed and irradiated samples, respectively [24]. The red shift can be predicted from the AFM images which can be further correlated with band gap study.

### 3.3. Raman spectroscopy studies

Raman scattering is a principal tool to investigate the vibrational states of a molecules in solid. Raman spectroscopy is also useful for the identification and crystal orientation properties of the materials [25]. Raman spectra of CdS–Bi<sub>2</sub>S<sub>3</sub> bi-layer thin film in the region 100–750 cm<sup>-1</sup> are recorded.

Fig. 4 shows the Raman spectra of CdS–Bi<sub>2</sub>S<sub>3</sub> thin films at room temperature. The spectra of the samples exhibit four distinct vibrational peaks at 121, 300 and 596 cm<sup>-1</sup>. All peaks corresponds to the longitudinal optical (LO)-phonon mode. The peak positions of CdS spectra are observed at 300 and 600 cm<sup>-1</sup> corresponding to 1LO (fundamental frequency) and 2LO (first overtone) phonon mode [26,27]. The peak position for Bi<sub>2</sub>S<sub>3</sub> is observed at 121 cm<sup>-1</sup> corresponds to 1LO which is in well agreement with report [28]. Raman spectra shows the dominant peaks of CdS as compared to Bi<sub>2</sub>S<sub>3</sub>, due to the excitation wave length of 514.5 nm, which is closely match with energy of first energy absorption band (2.48 eV) of CdS as compared to Bi<sub>2</sub>S<sub>3</sub> (1.72 eV). The FWHM of the annealed and irradiated samples is found to decreased. The change in FWHM is closely related to the diameter of nanocrystals [29]. The annealing and irradiation effect induces the growth in crystallite size, which is also confirmed from Raman study.

### 3.4. Optical studies

The energy band gap of as-deposited, annealed and Au<sup>9+</sup> irradiated thin films were studied by optical absorption. The band gap of samples was calculated by plotting graph between  $(\alpha h\nu)^2$  against the photon energy  $h\nu$ , with help of optical absorbance where  $\alpha$  is the absorption coefficient,  $h$  is the Plank constant and  $\nu$  is the frequency of incident light. Using Tauc's relation is given by



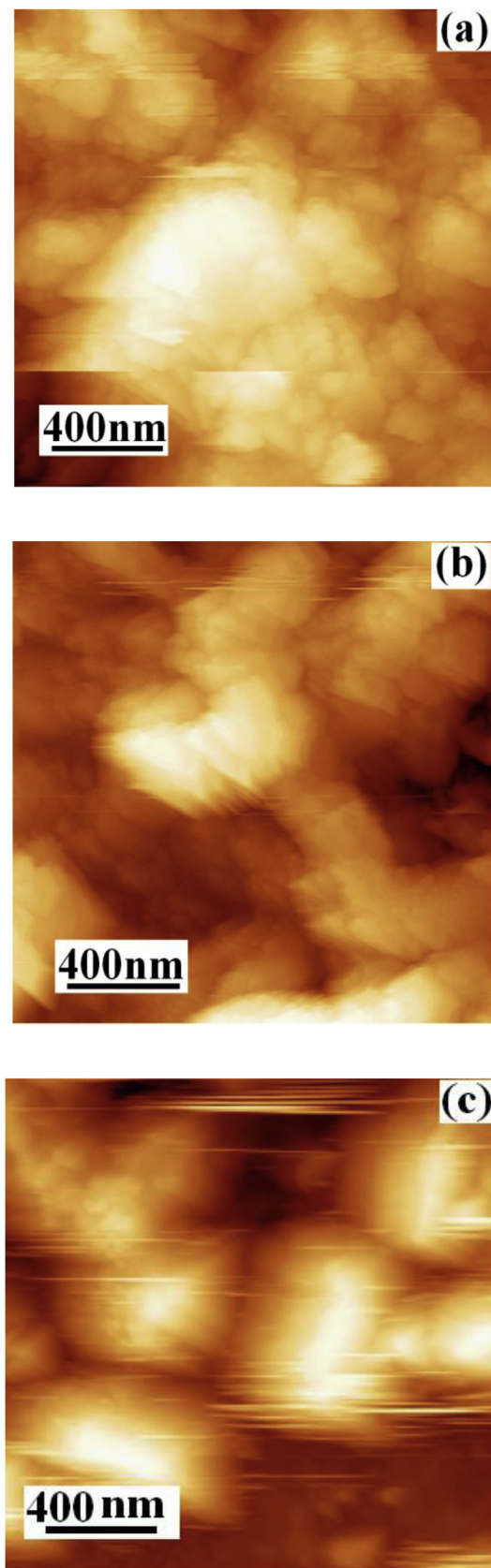


Fig. 3. AFM images of CdS–Bi<sub>2</sub>S<sub>3</sub> thin film (a) as-deposited, (b) 250 °C air annealed (c) irradiated samples at  $5 \times 10^{11}$  ion/cm<sup>2</sup> fluence.

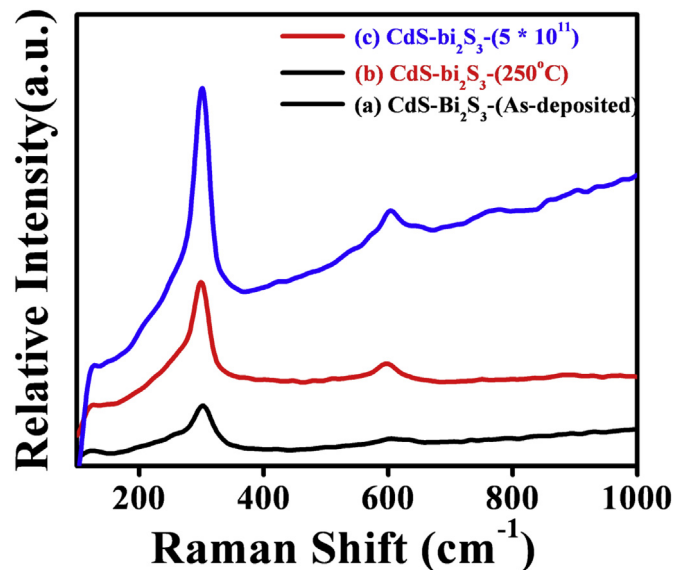


Fig. 4. Raman Spectra of as-deposited, annealed and irradiated samples.

$$\alpha = \frac{\alpha_0 (h\nu - E_g)^n}{h\nu} \quad (2)$$

where  $E_g$  the energy difference between valence and conduction band and  $n$  is a constant equal to  $1/2$  for direct band gap materials and  $2$  for indirect band gap material. The natures of the plots indicate the existence of direct transitions. The band gap  $E_g$  is determined by extrapolation of the straight portion of the plot to the energy axis as shown in Fig. 5(B). The absorbance spectra are studied at room temperature. The change in absorption is clearly observed in Fig. 5(A). The shift is observed towards the higher wavelength, indicating reduction in optical band gap at particular annealing temperature and irradiation fluence.

The obtained band gap of as-deposited thin film is  $1.81$  eV which, ranges between the band gap of CdS and Bi<sub>2</sub>S<sub>3</sub>. Annealing and irradiation reduces the band gap from  $1.59$  to  $1.48$  eV. The band gap is closely related with crystallite size [30–32]. The decrease in band gap indicates the red shift. The possible phenomenon in optical band gap of chalcogens was reported [33]. The decrease in band gap due to annealing can be correlated with agglomeration process which reduces the defects. In the case of irradiated samples the high energy ions result in bond breaking of atom which induces lattice damage and creates defect energy levels below the conduction band called as intermediate energy levels [34–36].

### 3.5. Electrical studies

In the electrical properties resistivity of the samples were studied by variation of the temperature using two probe method. Fig. 6 shows the variation of logarithm of electrical resistivity ( $\log \rho$ ) with the reciprocal of temperature ( $1/T$ ) for the samples. The electrical resistivity of as-deposited sample is expected to be higher than the irradiated sample. Electrical resistivity of the as-deposited sample is  $2.9 \times 10^{-3} \Omega\text{cm}$  reduces to  $2.1 \times 10^{-3} \Omega\text{cm}$  and  $1.6 \times 10^{-3} \Omega\text{cm}$  for annealed and irradiated samples, respectively. The decrease in resistivity after annealing and gold ion irradiation is due to increase in the crystallite size of the sample. The heavy ions induces grain growth as reported by the Alexandar and Was [37]. The activation energy was calculated by using following formula

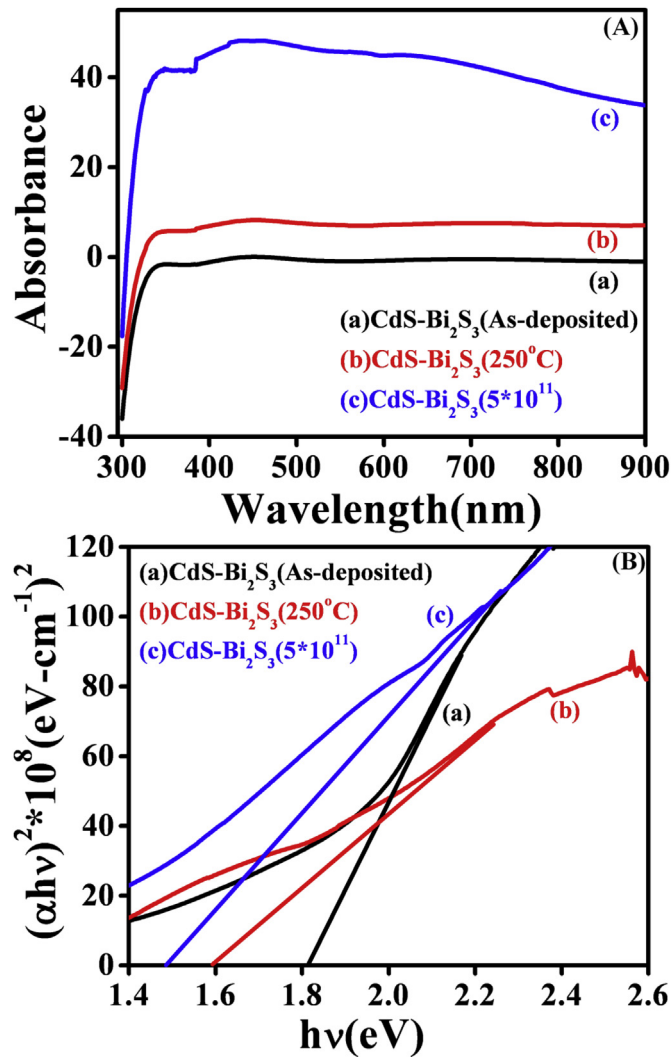


Fig. 5. The Plot of variation of  $(\alpha hv)^2$  versus  $(hv)$  (A) Optical absorbance (B) Energy band gap for all samples.

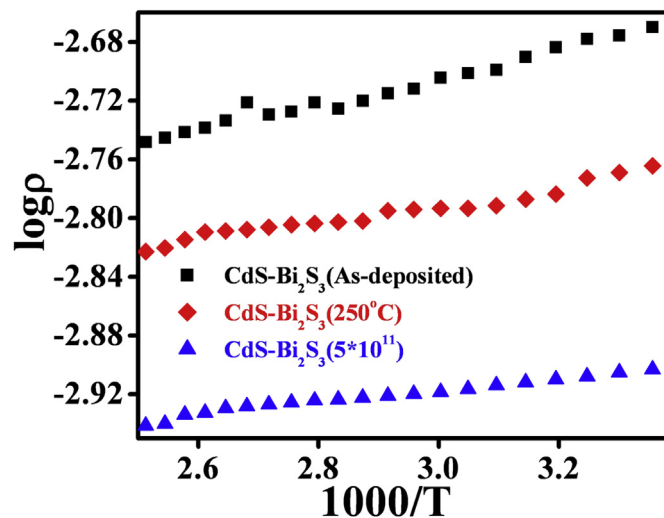


Fig. 6. Repetitive graph of  $1000/T$  versus  $\log \rho$  for resistivity of as-deposited, annealed and irradiated sample.

$$E_a \text{ (in eV)} = 2.303 \times k \times \text{slope}$$

where,

$E_a$  = Activation energy in electron volt.

$K$  = Boltzman's Constant ( $8.6 \times 10^{-5}$  eV/K).

The calculated values of activation energy are  $18 \times 10^{-3}$  eV,  $12 \times 10^{-3}$  eV and  $8 \times 10^{-3}$  eV for as-deposited, annealed and irradiated samples, respectively. The decrease in the resistivity and activation energy for annealed and irradiated samples might be due to reduction of the grain boundaries shown in AFM images. The grain boundaries create the electronic contact all over the thin film, which results in improved motion of electrons and intermediate energy level induced by irradiation [38].

### 3.6. Photosensitivity

The I–V characteristic of bi-layer thin film was studied with the help of Current-Voltage measurement system, at room temperature. On illumination of light the current in the samples is found to increase in the as-deposited, annealed and irradiated sample, respectively. In general the photocurrent generated by charge carriers increases with the intensity of the incident light. The excitation of valence electrons into conduction band improves the electrical conductivity of the semiconductor. This phenomenon is known as photo conductivity. Increase in the intensity of incident light causes increase in number of free carriers.

Fig. 7 (a), (b) and (c) shows the photo conductivity of as-deposited, annealed and irradiated samples, which was studied by the I–V graph in dark and under the illumination of 60 Watt light. The I–V Characteristics shows the diode like behavior. All sample showed good response for light. The photosensitivity of sample in the presence of light was calculated by the formula [20,39–42].

$$S = \frac{R_d - R_l}{R_d}$$

where

$R_d$  = resistance of thin film in dark

$R_l$  = resistance of thin film in the presence of light

The photosensitivity is found to be increased due to annealing and irradiation process, which can be correlated to increase in crystallite size and roughness in the surface of the samples after annealing and irradiation giving rise to increase in surface area which provides hefty space for light trapping as compared to as-deposited sample calculated with the help of XRD and AFM data. The decrease in the resistivity is due reduction of defects, which also supports the enhancement of photosensitivity. The calculated value of photosensitivity is 0.32, 0.43 and 0.54 for as-deposited, annealed and irradiated samples, respectively. The resultant effect is decrease in dark current and increase in photocurrent [43,44].

## 4. Conclusions

Chemically deposited CdS–Bi<sub>2</sub>S<sub>3</sub> bi-layer thin film is modified by an air annealing and irradiation. Annealing and irradiation process induces enhancement in crystallite size which, leads to decrease in the dislocation densities, resistivity, activation energy and band gap. The I–V graph shows increase in photo current when light of 60Watt intensity is incident on samples. The CdS–Bi<sub>2</sub>S<sub>3</sub> bi-

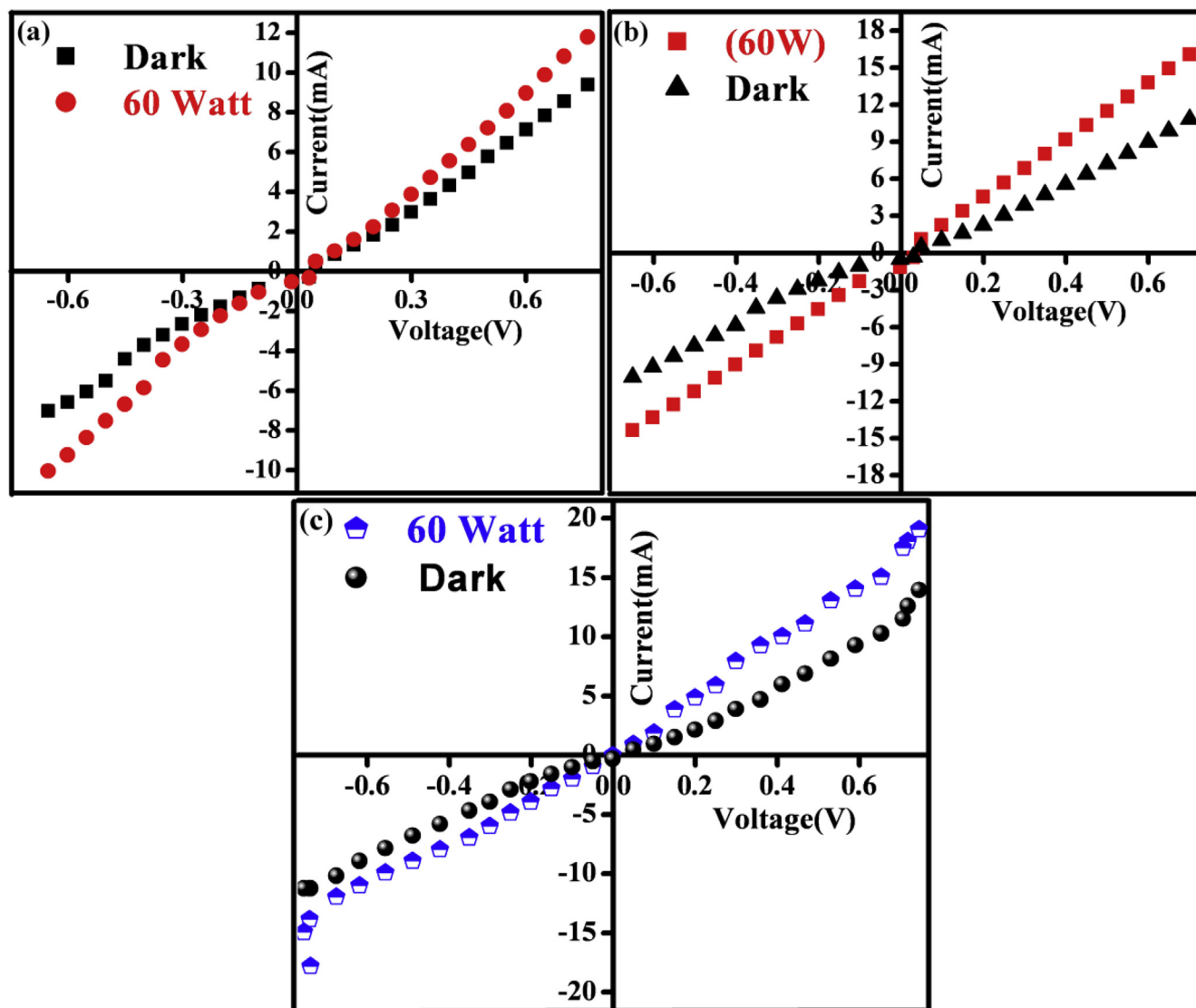


Fig. 7. IV graph of (a) as-deposited, (b) 250 °C air annealed (c) irradiated sample.

layer thin films are found to be stable against irradiation. The engineered CdS–Bi<sub>2</sub>S<sub>3</sub> bi-layer thin films can be used in photo-sensor and optoelectronic application.

#### Acknowledgements

Authors acknowledge, UGC-DAE Consortium of Scientific Research Indore for providing fellowship and financial support in the form of research project Ref. No: F No CSR-I/CRS-56. We are thankful to the Director, IUAC, New Delhi, and Dept. of Physics Dr.B.A.M. University Aurangabad for providing lab facilities. Special thanks to Dr. N.P.Lalla and Dr.Ganeshan for characterizations.

#### References

- [1] C. Thanachayanont, K. Inpor, S. Sahasithiwat, V. Meeyoo, J. Korean. Phys. Soc. 52 (2008) 1540–1544.
- [2] G. Sasikala, P. Thilakan, C. Subramanian, Sol. Energy Mater. Sol. Cell. 62 (2000) 275–293.
- [3] C.S. Ferekides, D. Marinsky, V. Viswanathan, B. Tetali, V. Palekis, P. Sevaraj, D.L. Morel, Thin Solid Film. 361 (2000) 520–526.
- [4] J. Pouzet, J.C. Bernede, A. Kellil, H. Essaidi, S. Benhida, Thin Solid Film. 208 (1992) 252–259.
- [5] J.S. Curran, R. Phillippe, Stresa, in: In Proceedings of the 14th International Conference on ECPV Solar Energy, 1982, pp. 10–14.
- [6] G. Ghosh, B.P. Varma, Solid State Commun. 31 (1979) 683–687.
- [7] G. Ghosh, B.P. Varma, Thin Solid Film. 60 (1979) 61–65.
- [8] R.R. Ahire, B.R. Sankpal, C.D. Lokhande, Mater. Chem. Phys. 72 (2001) 48–55.
- [9] R.R. Ahire, N.G. Deshpande, Y.G. Gudage, A.A. Sagade, S.D. Chavan, D.M. Phase, R. Sharma, Sens. Actuators A Phys. 140 (2007) 207–214.
- [10] A. Naveen, S. Mitesh, C.J. Panchal, Invertis J. Renew. Energy 4 (2014) 121–126.
- [11] R. Lisha, T. Hysen, P. Geetha, P.B. Aravind, M. Shareef, A. Shamlath, O. Sunil, R.V. Ramanujan, M.R. Anantharaman, Nucl. Instrum. Meth. B 360 (2015) 68–74.
- [12] G.K. Williamson, R.E. Smallman, Philos. Mag. 1 (1956) 34–45.
- [13] P. Kumar, N. Jain, R.K. Agrawal, Chalcogenide Lett. 7 (2010) 89–94.
- [14] D.C. Agarwal, K. Amit, S.A. Khan, D. Kabiraj, F. Singh, A. Tripathi, J.C. Pivin, R.S. Chauhan, D.K. Avasthi, Nucl. Instrum. Methods Phys. Res. Sect. B 244 (2006) 136–140.
- [15] S. Chandramohan, R. Sathyamoorthy, P. Sudhagar, D. Kanjilal, D. Kabiraj, K. Asokan, V. Ganesan, T. Shripathi, U.P. Deshpande, Appl. Phys. A 94 (2009) 703–714.
- [16] S.U. Shaikh, D.J. Desale, F.Y. Siddiqui, G. Arindam, R.B. Birajadar, A.V. Ghule, R. Sharma, Mater. Res. Bull. 47 (2012) 3440–3444.
- [17] G.K. Padam, G.L. Malhotra, S.U.M. Rao, J. Appl. Phys. 63 (3) (1988) 770–774.
- [18] R.R. Ahire, A.A. Sagade, S.D. Chavhan, V. Huse, Y.G. Gudage, F. Singh, D.K. Avasthi, D.M. Phase, R. Sharma, Curr. Appl. Phys. 9 (2009) 374–379.
- [19] P.M. Ratheesh, C. Kumar, K. Sudha, K.P. Vijayakumar, J. Appl. Phys. 97 (2005) 013509–013515.
- [20] R.R. Ahire, A.A. Sagade, N.G. Deshpande, S.D. Chavhan, R. Sharma, F. Singh, J. Phys. D. Appl. Phys. 40 (2007) 4850–4854.

- [21] A. Dumbrava, C. Badea, A.G. Prodan, V. Ciupina, *Chalcogenide Lett.* 7 (2010) 111–118.
- [22] K.K. Nanda, F.E. Kruis, H. Fissan, *Phys. Rev. Lett.* 89 (2002), 256103–256104.
- [23] S. Ghosh, S.A. Khan, V. Ganesan, S. Kundu, R. Bhattacharya, *Nucl. Instrum. Methods B* 244 (2006) 34–39.
- [24] N.G. Deshpande, A.A. Sagade, S.D. Chavhan, J.C. Vyas, F. Singh, A.K. Tripathi, D.K. Avasthi, R. Sharma, *Vacuum* 82 (2007) 39–44.
- [25] K. Soumitra, C. Subhadra, *J. Phys. Chem. B* 110 (2006) 4542.
- [26] L. Zeiri, I. Patla, S. Acharya, Y. Golan, S. Efrima, *J. Phys. Chem. C* 111 (2007) 11843–11848.
- [27] R.P. Rajeev, M.K. Abdul, *Bull. Mater. Sci.* 31 (2008) 511–515.
- [28] Y. Xuelian, C. Chuanbao, *Cryst. Growth Des.* 8 (2008) 3951–3955.
- [29] P. Nandakumara, C. Vijayan, M. Rajalakshmi, A.K. Arora, Y.V.G.S. Murti, *Phys. E* 11 (2001) 377–383.
- [30] Y. Kayanuma, *Phys. Rev. B* 38 (1988) 9797–9805.
- [31] C.Q. Sun, X.W. Sun, B.K. Tay, S.P. Lau, H. Huang, S. Li, *J. Phys. D.* 34 (2001) 2359–2362.
- [32] S. Chowdhury, S.K. Dolui, D.K. Avasthi, A. Choudhury, *Indian J. Phys.* 79 (2005) 1019–1022.
- [33] M.S. Kamboj, G. Kaur, R. Thangaraj, D.K. Avasthi, *J. Phys. D. Appl. Phys. Lett.* 35 (2002) 477–482.
- [34] Y.S. Chaudhayr, S.A. Khan, R. Shrivastava, V.R. Satsangi, S. Prakash, D.K. Avasthi, S. Dass, *Nucl. Instr. Meth. B* 225 (2004) 291–296.
- [35] S. Soundeswaran, O. Senthil Kumar, P. Ramasamy, D. Kabi Raj, D.K. Avasthi, R. Dhanasekaran, *Phys. B* 355 (2005) 222.
- [36] S. Chandramohan, R. Sathymoorthy, P. Sudhagar, D. Kanjilal, D. Kabiraj, K. Asokan, *Nucl. Instrum. Methods B* 254 (2007) 236–242.
- [37] D.E. Alexander, G.S. Was, *Phys. Rev. B* 47 (1993), 2983.
- [38] B.R. Sankapal, C.D. Lokhande, *Mater. Chem. Phys.* 74 (2002) 126.
- [39] S. M. Sze, *John Wiley and Sons*, New York, 1994, pp. 67.
- [40] Sharma Ramphal, C. Gangri, V.S. Dipak, S.A. Patil, S. Shaheed, V.G. Anil, S.M. Rajaram, H. Sung-Hwan, *J. Mater. Chem. C* 2 (2014) 8012.
- [41] L. Fangyuan, Y. Juehan, L. Renxiong, H. Nengjie, L. Yongtao, W. Zhongming, L. Jingbo, *J. Mater. Chem. C* 2 (2014) 5836.
- [42] X. Wei-Wei, C. Jin-Qiang, W. Xing-Cai, Z. Jun-Jie, *J. Mater. Chem. C* 2 (2014) 7392, <http://dx.doi.org/10.1039/C4TC02492C>.
- [43] F.B. Micheletti, P. Mark, *Appl. Phys. Lett.* 10 (1967) 136–138.
- [44] J.W. Orton, B.J. Goldsmith, J.A. Chapman, M.J. Powell, *J. Appl. Phys.* 53 (1982) 1602–1614.